Time-Domain Optical Sampling of Switched-Mode Microwave Amplifiers and Multipliers

Manoja D. Weiss, *Student Member, IEEE,* Matthew H. Crites, Eric W. Bryerton, *Member, IEEE,* John F. Whitaker, *Member, IEEE,* and Zoya Popović, *Senior Member, IEEE*

***Abstract*— Time-domain measurements of the output waveforms of two 8-GHz high-efficiency power amplifiers, a 1-GHz frequency doubler, and a 5-GHz frequency doubler are presented in this paper. A new photoconductive probe has enabled nonintrusive time-domain voltage measurements, which confirm switched-mode class-E and class-F amplifier operation. In order to analyze nonlinear amplifiers designed to deliver a sinusoidal wave to the load, voltages at characteristic points inside the circuit need to be known. In multipliers, waveform measurements track harmonic leakage, expediting the design cycle. The high-impedance probe used here is an optoelectronic sampler, which can sense the charge on an exposed interconnect or the field associated with a buried interconnect. These electric-field data are then converted into voltage.**

***Index Terms*— High efficiency, power amplifiers, optical sampling, transistor multipliers.**

I. Introduction

IN HIGH-EFFICIENCY class-E and class-F power amplifiers, the transistor is used as a switch and the harmonics of the switched voltage are reflected back toward the transistor before reaching the load, such as has been demonstrated in the megahertz range [1]–[3]. This is usually accomplished by the use of matching circuits and filters, and produces switch current and voltage waveforms that are exactly out of phase with each other. The losses within the switching transistor are thus minimized. If large signal models of the transistor are available, the time-domain waveforms at the switch can be simulated using harmonic balance methods to demonstrate the offset between the current and voltage waveforms. In [4], such simulations are used in the design of microwave power amplifiers. In this paper, we present frequency scaling of class-E and class-F amplifiers to X-band.

High-efficiency circuits can also be used to produce frequency doubling. This is done by reflecting the fundamental back to the transistor and presenting the second harmonic with a suitable load that will give out-of-phase switch voltage and current waveforms. Again, harmonic balance simulation methods can be used to demonstrate this offset between waveforms. This paper presents the design and performance of two switched-mode microwave transistor multipliers.

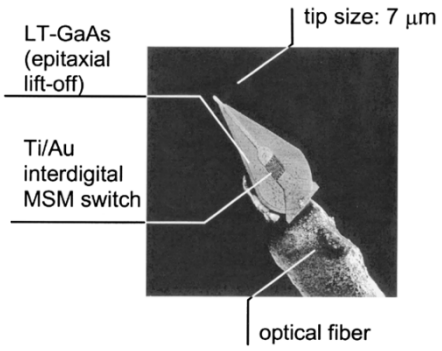

Fig. 1. Micromachined photoconductive probe with optical fiber.

One verification of class-E or class-F performance is simply obtaining high efficiency while maintaining high output power. However, this leaves an ambiguity in the specific class of operation of the circuit and, therefore, does not validate the design. In the case of multiplier circuits, output power and frequency measurements are used to ascertain proper circuit operation. Knowledge of the switch waveform would significantly add to the understanding of circuit performance and the ability to improve the design.

At low frequencies (up to about 500 MHz), the switch voltage can be measured by introducing a large resistor between the drain and source and measuring the voltage across this resistor using an oscilloscope [5]. At higher frequencies, it is not possible to measure these waveforms due to the difficulty in making high-impedance probes at these frequencies. Recent advancements in photoconductive probing of microwave circuits [6], [7] have paved a way to nonintrusively measure such voltage waveforms up to very high frequencies.

II. Photoconductive Probing

The photoconductive probe utilized in the time-domain measurement of the high-efficiency amplifier response is a micromachined optical-fiber-coupled optoelectronic sampling head [8]–[10]. Shown in Fig. 1, the probe head itself utilizes a 1.5-μm-thick substrate layer of GaAs, which was grown epitaxially at 200 °C (so-called low-temperature GaAs) and then annealed at 600 °C. The GaAs layer prepared in this

Manuscript received March 26, 1999; revised July 9, 1999. This work was supported by the Air Force Office of Scientific Research, Air Force Materiel Command, under Grant F49620-98-1-0365, by the National Science Foundation, Center for Ultrafast Optical Science, under Grant STC PHY 8920108, and by Caltech, Army Research Office Multidisciplinary Research Initiative Program on Quasi-Optical Power Combining under Grant DAAH04-96-10001.

M. D. Weiss, E. W. Bryerton, and Z. Popović are with the Department of Electrical and Computer Engineering, University of Colorado, Boulder, CO 80309 USA.

M. H. Crites and J. F. Whitaker are with the Department of Electrical Engineering, The University of Michigan at Ann Arbor, Ann Arbor, MI 48109 USA.

Publisher Item Identifier S 0018-9480(99)08461-6.

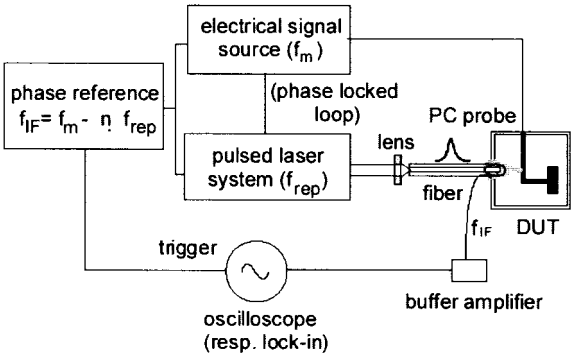

Fig. 2. Optical sampling measurement setup.

fashion has a 1-ps carrier relaxation time (thus, the sampling gate was active for only a brief time), a resistivity of 10^7 Ω·cm (so the photogate would have high off-state resistance), and a breakdown voltage of nearly 10^6 V/m. The photogate consisted of a 30 μm $\times$ 30 μm gold pattern of interdigitated fingers, which are 1.5 μm in width with 1.5-μm separations. The probe, with its 7-μm-wide tip, which extends out past the GaAs for contacting circuit metallizations, can sense the potential on an exposed interconnect or the field associated with a buried interconnect. A photocurrent proportional to the potential within the sampling window is then generated at the photogate before being converted back into a voltage signal.

The current to voltage conversion is accomplished by a JFET source follower circuit [11] with an input resistance of 1 TΩ and an input capacitance of 3 pF. This high input resistance avoids charge drainage from the device-under-test so that measurement with minimal invasiveness is achieved. Due to the small amount of charge necessary to load the source follower input, the actual voltage level is built up in a short time, allowing a higher modulation bandwidth and the ability to measure absolute voltage levels. In addition, the high input resistance of the source follower allows the instantaneous dc voltage at the probe node to be determined at the output of the source follower and, thus, both ac and dc signals can be measured simultaneously.

In this measurement system, shown in Fig. 2, the probe is illuminated by a train of femtosecond-duration laser pulses, and the output voltage is recorded on a low-frequency oscilloscope. The output voltage is a down-converted replica of the unknown microwave signal. If a frequency-domain output is required, a lock-in amplifier or a spectrum analyzer can be used in place of the oscilloscope. For an unknown microwave signal with frequency f_m, heterodyne mixing and equivalent time-sampling dictate that the following relationship between the microwave and intermediate frequencies be fulfilled:

$$f_m = n f_{\rm rep} \pm f_{\rm IF} \tag{1}$$

where n is an integer and $f_{\rm rep} = 80$ MHz is the laser pulse repetition frequency. The intermediate frequency $f_{\rm IF}$ is typically in the kilohertz range and provides a replica of the unknown microwave signal. The Ti:sapphire laser used in this system is phase locked to the microwave source so that the in-circuit electrical signal can be determined in amplitude and phase. The probe has a 3.5-ps time response, which relates to a bandwidth over 100 GHz. Therefore, the probe should exhibit a frequency response which extends into the millimeter-wave region.

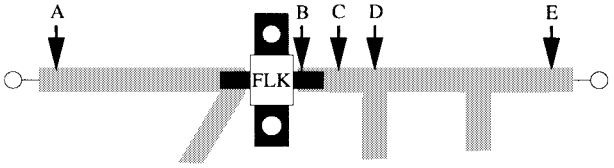

Fig. 3. General outline of class-E and class-F amplifier circuits showing locations of optical probing.

III. Photoconductive Probing of High-Efficiency Amplifiers

The two amplifiers are built on RT Duroid substrates with $\epsilon_r = 2.2$ and 0.508-mm thickness. The general outline of the two circuits is given in Fig. 3. The input to the amplifiers is at point **A**, and **E** is the output. Harmonics generated at the drain are reflected back to the input through the feedback capacitance $C_{\rm gd}$ between the device gate and drain, resulting in reduced efficiency of the amplifier. The input circuit, in addition to performing a matching function, must also filter these reflected harmonics. The output circuit also filters out harmonics as well as providing the correct loading to the transistor at the fundamental frequency. The points at which the circuit is probed are shown as **A**, **B**, **C**, **D**, and **E** in Fig. 3 and correspond to plots given in this paper. The gate and drain gold leads are soldered to the rest of the circuit so that an exposed gold area exists for the probe to make contact with.

The measured waveform amplitudes cannot be used to calculate power since the local impedance is unknown. However, they are very useful in analyzing the harmonic content of the waveform. Point **A** represents the input plane of the amplifier. Ideally, the input circuit filters out any harmonics reflected to the gate from the drain, and the voltage at this point is a sine wave. Point **B**, representative of the switch voltage, is on the gold drain lead of the package, as close to the transistor as the probe can be positioned, and indicates the class of operation of the amplifier. This waveform is not identical to the switch voltage due to package output parasitics, especially the small lead inductance. We estimate from measurement the package lead inductance to be about 0.25 nH. The effect of this series parasitic element is an increase of about 10–20 ps in rise and fall times of an ideal square wave at the intrinsic device output. This means that the waveform at the intrinsic device leans more toward the rising edge compared to the waveform measured at **B**. The waveforms at **C**, **D**, and **E** are helpful in analyzing the filtering functions of the output circuit. The voltage at **E** should be a sine wave if proper filtering is taking place.

A. Class-F Nonlinear Amplifier

1) Design: Class-F amplifier design requires an output impedance given by

$$Z_L = \frac{V_{\rm dd}}{2I_{\rm dss}} \tag{2}$$

at the fundamental switching frequency [12], to present a short circuit at all even harmonics and an open circuit at

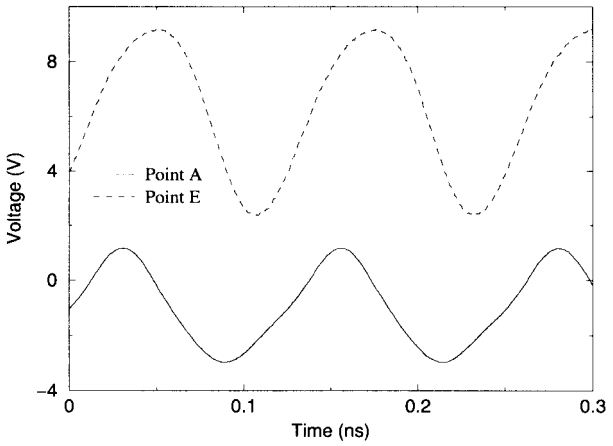

Fig. 4. Optically sampled waveforms at points **A** and **E** in the class-F circuit, corresponding to the input and output respectively. The input and output waveforms are both sinusoidal signals.

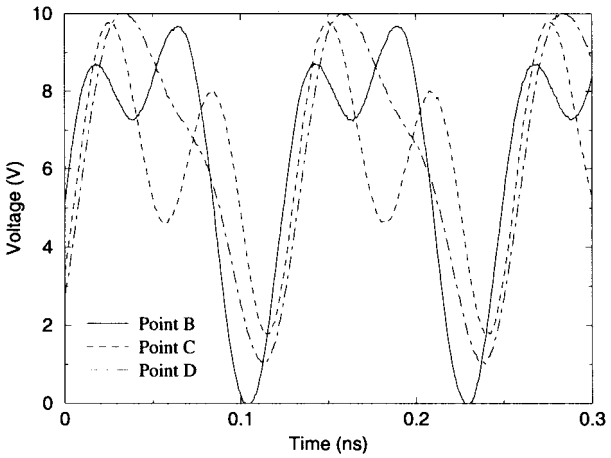

Fig. 5. Optically sampled waveforms at points **B**, **C**, and **D** in the class-F circuit. In the switch waveform at **B**, the fundamental and third harmonic approximate a square wave. At **C**, which is before the second harmonic shorting stub, there is a significant second harmonic component, and at **D**, the harmonics have mostly been filtered out. These waveform amplitudes cannot be used to calculate power since the local impedance is unknown.

all odd harmonics. $V_{\rm dd}$ and $I_{\rm dss}$ are the drain bias voltage and the maximum current of the transistor, respectively. The impedance given by (2) provides maximum power transfer between the transistor and output. The voltage at the switch of a class-F amplifier is a square wave because the voltage contains negligible second harmonic content, but significant third harmonic contribution. The amplifier is built with the Fujitsu FLK052WG packaged MESFET previously used at C-band and presented in [4]. Electrical measurements at 8.0 GHz show a drain efficiency of 73%, a power-added efficiency (PAE) of 61%, and 28.6-dBm output power. The input power was 22 dBm. Harmonic balance simulations of the waveforms were not possible because a large-signal model for the transistor was not available.

2) Optical Time-Domain Measurements: The input waveform measured at point **A** in Fig. 3 is a sinusoidal waveform biased at about -1.0 V, as shown in Fig. 4. Since there are very little harmonics in the waveform at **A**, we can conclude that there is no significant harmonic content being reflected back to the input of the amplifier.

Fig. 5 shows the voltage waveforms at points **B**, **C**, and **D** in Fig. 3. The waveform at **B** shows the square shape of the switch voltage, which is consistent with class-F operation. The two peaks in the waveform are due to the fundamental frequency and the third harmonic, as is evidenced by the spacing between peaks. The second harmonic does not appear in this waveform since it is presented with a short at the output. Higher harmonics are not present because the transistor does not have gain at these harmonic frequencies.

However, in Fig. 5, it is evident that there is a significant second harmonic contribution at point **C** (Fig. 3). This is due to the standing wave between the transistor output and the first stub, which provides the second harmonic short.

As shown in Fig. 5, the second harmonic is not strong in the waveform at point **D**. The distortion in the waveform indicates that there is some second harmonic leakage beyond the first stub.

Beyond the second output stub, at point **E**, the output waveform is sinusoidal. This is shown in Fig. 4 along with the input waveform for comparison. This is part of the design of a class-F circuit, in which the output circuit must filter out the harmonics in the switched waveform. These measurements verify the proper waveforms inside the power amplifier and, therefore, substantiate the class-F design.

B. Class-E Nonlinear Amplifier

1) Design: Transmission-line class-E amplifiers require the fundamental load impedance to be given by

$$Z_L = \frac{0.28015}{2\pi f_s C_s} e^{j49.0524^\circ} \tag{3}$$

where f_s is the fundamental frequency, and C_s is the transistor switch output capacitance approximated by $C_{\rm ds}$. All harmonics are terminated in an open circuit [13], [4]. This is determined by specified boundary conditions in the time domain.

The value of $C_{\rm ds}$ to be used in the class-E amplifier design is deembedded from low-frequency s-parameters. Since $C_{\rm ds}$ is a geometry-based capacitance, this is a reasonable approximation for the switch capacitance, even though the nonlinear capacitance $C_{\rm gd}$ affects the total output capacitance. The lack of a large-signal model for this transistor prohibits waveform simulations that would aid in the design of these circuits. The class-E amplifier is built with the Fujitsu FLK202MH-14 packaged MESFET, which has a gate periphery four times larger than the FLK052.

Power measurements result in a drain efficiency of 64%, PAE of 48%, and 31.5-dBm output power at 8.35 GHz. The optical measurements were made at 8.32 GHz since the microwave frequency must be a multiple of the laser repetition frequency of 80 MHz according to (1).

2) Optical Time-Domain Measurements: For the class-E circuit, only voltages at points **B** and **E** in Fig. 3 are shown since they are the salient waveforms of class-E operation.

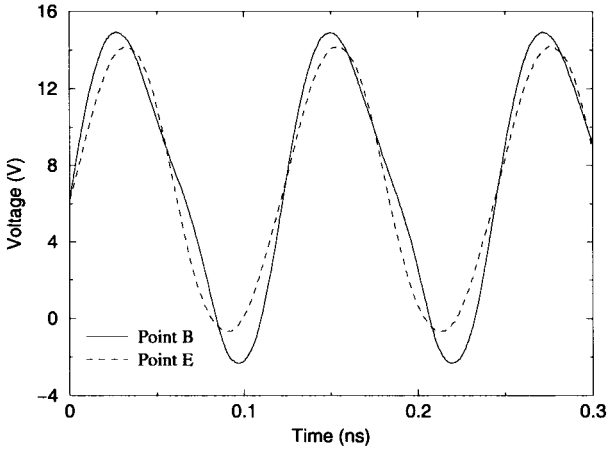

Fig. 6. Measured waveforms at points **B** and **E** in the class-E circuit. The shape of the voltage wave at **B** is similar to that in Fig. 6, with a second harmonic component in the waveform. The output wave at **E** is sinusoidal.

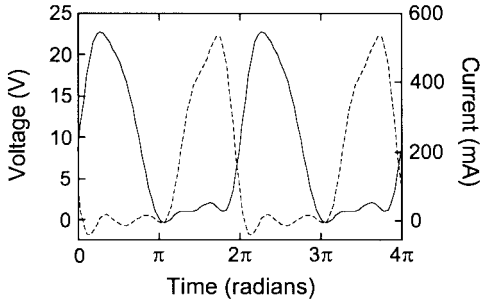

Fig. 7. Simulated waveform of a 500-MHz class-E circuit using a Materka–Kacprzak nonlinear model for a Siemens CLY5 MESFET. The solid line signifies voltage and the dashed line denotes current.

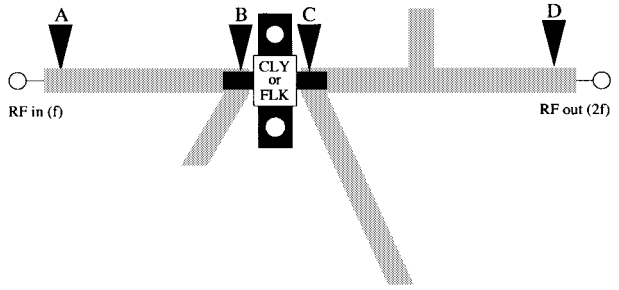

Fig. 8. General layout of frequency doublers showing locations of optical probing.

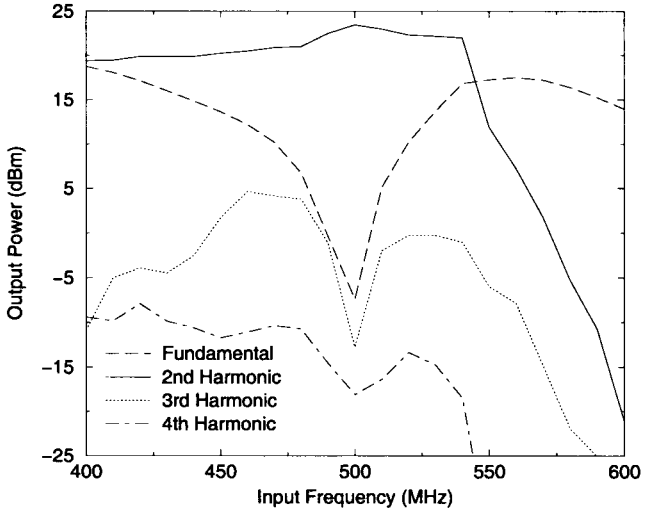

Fig. 9. Measured output power at the fundamental and first three harmonics versus input frequency for the 1-GHz doubler ($P_{\rm in} = 15$ dBm, $V_{\rm DS} = 5$ V, and $I_{\rm DS} = 110$ mA).

Fig. 6 shows the voltage at point **B**, which is the voltage waveform across the switch. For comparison, a harmonic balance simulation at 500 MHz for a different class-E amplifier [14] is shown in Fig. 7. A suitable nonlinear model was available for this MESFET (Siemens CLY5). The switch voltage waveform in this case is not square, but has considerable fundamental and second harmonic content, giving it the shape of a narrow left-hand-side-skewed half-sinusoid. The measurement also shows the second harmonic portion of the waveform, which produces the left-hand-side-skewed voltage wave. The simulated voltage is close to zero for nearly half of the period, approaching ideal class-E operation. The measured voltage, however, is not flat in this half of the period, resulting in a higher vi product (loss). This is consistent with nonoptimal class-E operation since the circuit is operated above the critical frequency for class-E operation, in this case, about 1.5 GHz [4], [15]. The measured class-E waveform is very different from the class-F switch voltage in Fig. 5, which depicts a square wave consisting of the fundamental and third harmonic.

At point **E**, the filtered output waveform appears as a sinusoidal pattern, as shown in Fig. 6. This analysis verifies that the power amplifier is indeed operating in the desired class-E mode.

IV. Photoconductive Probing of High-Efficiency Doublers

Frequency multiplication is commonly used in millimeter-wave transmitter systems [16]–[18]. Including a frequency multiplier allows the oscillator to operate at a submultiple of the output frequency resulting in a cheaper, cleaner, and more stable oscillator. Also, operation of the oscillator and high-power stages at different frequencies reduces the effects of feedback. An amplifier chain is typically required in millimeter-wave systems to compensate for the losses in the multiplier and to achieve the necessary output power. Zulinski showed that class-E multipliers can provide high-efficiency multiplication at high frequencies [19].

A 500-MHz to 1-GHz and a 2.5–5-GHz doubler were designed and measured. To perform the optical measurements, the doublers were tuned to 480–960 MHz and 2.56–5.12 GHz, respectively, in order to correspond to a multiple of the laser pulse repetition frequency.

Fig. 8 depicts the general layout of the doubler circuits. The first stub at the output is $\lambda/4$ long at the fundamental frequency, shorting the fundamental and odd harmonics, while passing the second harmonic. The second stub presents the impedance given by (3) to the second harmonic.

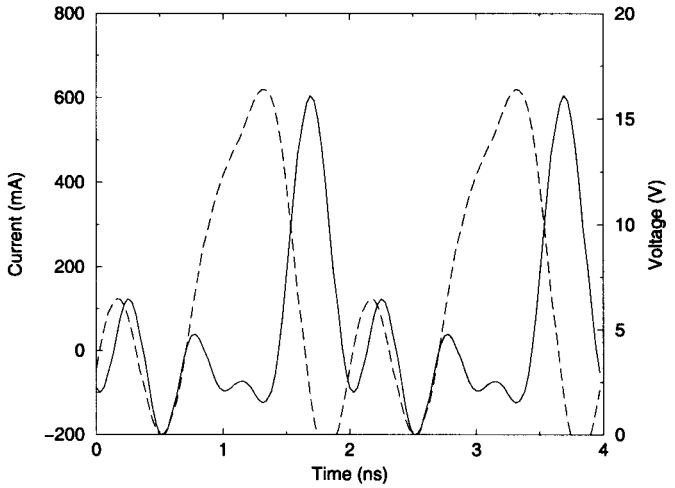

Fig. 10. Simulated drain voltage (solid line) and current (dashed line) waveforms for the 1-GHz doubler.

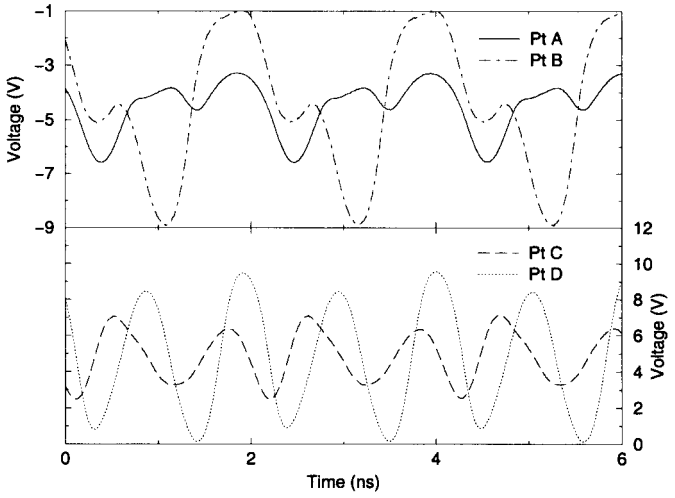

Fig. 11. Optically sampled waveforms at points **A**–**D** in the 480–960-MHz doubler.

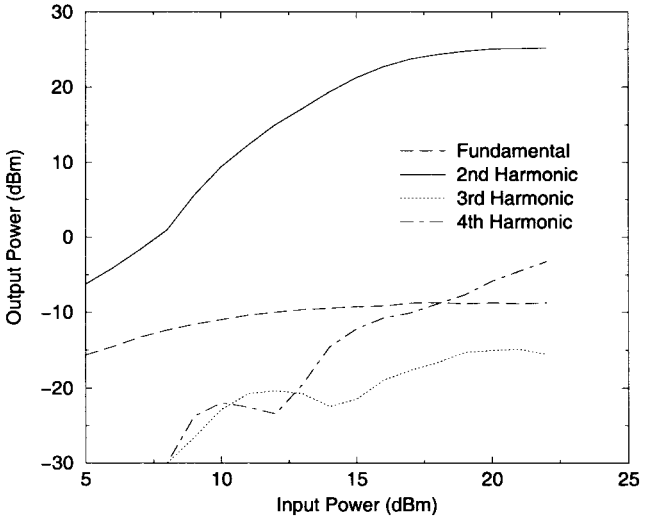

Fig. 12. Measured output power at the fundamental (2.5 GHz) and first three harmonics versus input power for the 5-GHz doubler ($V_{\rm DS} = 8$ V, and $I_{\rm DS} = 100$ mA).

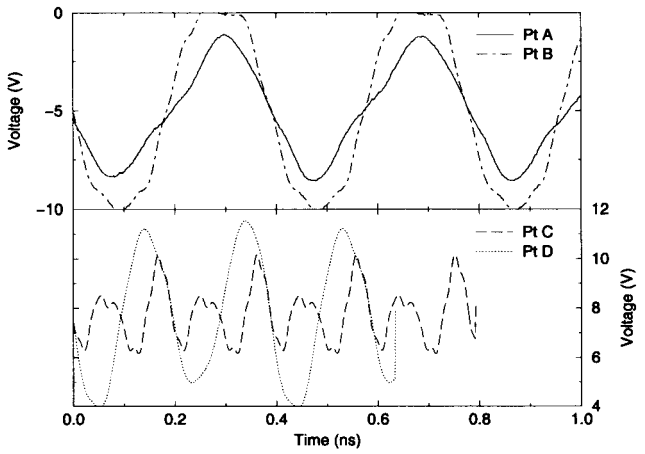

Fig. 13. Optically sampled waveforms at points **A**–**D** in the 2.56–5.12-GHz doubler.

A. 1-GHz Doubler

The 1-GHz doubler was fabricated in microstrip using the Siemens CLY5 MESFET ($C_{\rm ds} = 2.6$ pF). This device was also used to make class-E amplifiers at 0.5, 1, and 2 GHz [13]. A 500-MHz, 15-dBm input signal produced 23.5-dBm output power with 35% PAE and 40% drain efficiency at 1 GHz with greater than 30-dB rejection for the unwanted frequencies. A frequency sweep for this circuit is shown in Fig. 9.

A five-tone harmonic balance simulation was performed using a Materka model for the device and predicted 24.8-dBm output power, 43% drain efficiency (within 3% of the measured value), and 8.8-dB conversion gain. The simulated drain voltage and current waveforms in Fig. 10 exhibit characteristics resembling class-E operation; the slope of the current waveform is steeper on the falling edge than on the rising edge.

Time-domain measurements of the 1-GHz circuit are shown in Fig. 11. As shown, at both points **A** and **B**, there is significant harmonic content, especially third harmonic. This indicates that third harmonic power is being reflected back to the input. Based on these measurements, an improved design should include a third harmonic trap at the input. At point **D**, a fairly pure sine wave at the second harmonic is seen. At the drain, point **C**, some waveshaping is seen, but not enough to consider this class-E operation. More harmonic tuning is required at the output.

B. 5-GHz Doubler

A 5-GHz doubler was fabricated in microstrip using the Fujitsu FLK052WG MESFET ($C_{\rm ds} = 0.4$ pF). This device was also used to make a 5-GHz class-E amplifier [5] and oscillator [20]. A 2.5-GHz 20-dBm input signal produced 330-mW output power with 5.2-dB conversion gain and 29% PAE at 5 GHz. For input powers greater than 15 dBm, the rejection of the unwanted frequencies is greater than 30 dB. A power sweep for this doubler is shown in Fig. 12.

Fig. 13 shows the time-domain measurements of the 5-GHz doubler. At both input points, significant harmonic content is seen, showing the need for harmonic tuning at the input. At point **C**, fourth, sixth, and even eighth harmonics are seen in the waveform. With higher order harmonic tuning at the device output, class-E operation at the doubled frequency may

indeed be approached. At point **D**, the waveform has cleaned up significantly.

V. Conclusion

Optical sampling was used to examine the harmonic content of the voltage waveform at various characteristic points in several nonlinear microwave circuits. This information is vital in verifying the class of operation of high-efficiency switched-mode power amplifiers and multipliers since the specific class depends on the shape of the switch waveform. The class-F and class-E power amplifiers examined in this paper were found to operate in the correct mode. In the absence of good large-signal models for the Fujitsu power transistors used here, this optical sampling analysis substantiates the approximate design method based on small-signal parameters.

This measurement technique is shown to be valuable for design and analysis of microwave frequency multipliers. By measuring the harmonic content of the waveforms, it can be seen at which points in the circuits further harmonic tuning needs to be applied.

References

[1] N. O. Sokal and A. D. Sokal, "Class E—A new class of high-efficiency tuned single-ended switching power amplifiers," *IEEE J. Solid-State Circuits*, vol. SC-10, pp. 168–176, June 1975.

[2] H. L. Krauss, C. W. Bostian, and F. H. Raab, *Solid-State Radio Engineering*. New York: Wiley, 1980.

[3] J. F. Davis and D. B. Rutledge, "A low-cost class-E power amplifier with sine-wave drive," in *IEEE MTT-S Int. Microwave Symp. Dig.*, Baltimore, MD, June 1998, pp. 1113–1116.

[4] T. B. Mader, E. Bryerton, M. Marković, M. Forman, and Z. B. Popović, "Switched-mode high-efficiency microwave power amplifiers in a free-space power-combiner array," *IEEE Trans. Microwave Theory Tech.*, vol. 46, pp. 1391–1398, Oct. 1998.

[5] T. B. Mader, *Quasi-Optical Class-E Power Amplifiers*, Ph.D. dissertation, Dept. Elect. Comput. Eng., Univ. Colorado, Boulder, CO, 1995.

[6] G. David, K. Yang, M. Crites, J. S. Rieh, L. H. Lu, P. Bhattacharaya, L. P. B. Katehi, and J. F. Whitaker, "Photoconductive probing and computer simulation of microwave potentials inside a SiGe MMIC," presented at the Int. Topical Meeting Silicon Monolithic Integrated Circuits RF Syst., Ann Arbor, MI, Sept. 1998.

[7] G. David, T.-Y. Yun, M. H. Crites, J. F. Whitaker, T. R. Weatherford, K. Jobe, S. Meyer, M. Bustamante, B. Goyette, S. T. III, and K. R. Elliot, "Absolute potential measurements inside microwave digital IC's using a micromachined photoconductive sampling probe," *IEEE Trans. Microwave Theory Tech.*, vol. 46, pp. 2330–2337, Dec. 1998.

[8] J. Whitaker, "Optoelectronic applications of LTMBE III–V materials," *Mater. Sci. Eng.*, pp. 61–67, 1993.

[9] S. Gupta, J. Whitaker, and G. Mourou, "Ultrafast carrier dynamics in III–V semiconductors grown by molecular-beam-expitaxy at very low substrate temperatures," *IEEE J. Quantum Electron.*, vol. 28, pp. 2464–2472, Oct. 1992.

[10] J. Hwang, H. Cheng, J. Whitaker, and J. Rudd, "Modulation bandwidth and noise limit of photoconductive gates," *Opt. Quantum Electron.*, vol. 28, pp. 961–973, 1996.

[11] ———, "Photoconductive sampling with an integrated source follower/amplifier," *Appl. Phys. Lett.*, vol. 68, pp. 1464–1466, 1996.

[12] S. C. Cripps, "A theory for the prediction of GaAs FET load–pull contours," in *IEEE MTT-S Int. Microwave Symp. Dig.*, Boston, MA, June 1983, pp. 221–223.

[13] T. B. Mader and Z. B. Popović, "The transmission line class-E amplifier," *IEEE Microwave Guided Wave Lett.*, vol. 5, pp. 290–292, Sept. 1995.

[14] M. Markovic, A. Kain, and Z. Popović, "Nonlinear modeling of class-E microwave power amplifiers," *Int. J. RF Microwave Computer-Aided-Eng.*, vol. 9, pp. 93–103, Mar. 1999.

[15] F. H. Raab, "Suboptimum operation of class-E power amplifiers," in *Proc. RF Technol. Expo 89*, Santa Clara, CA, pp. 85–98.

[16] M. Funabashi, T. Inoue, K. Ohata, K. Maruhashi, K. Hosoya, M. Kuzuhara, K. Karekawa, and Y. Kobayashi, "A 60-GHz MMIC stabilized frequency source composed of a 30-GHz DRO and a doubler," in *IEEE MTT-S Int. Microwave Symp. Dig.*, Orlando, FL, May 1995, pp. 71–74.

[17] H. Meinel, "Millimeter-wave opportunities for automotive and radio applications," presented at the IEEE MTT-S Int. Microwave Symp. Workshop, Denver, CO, June 1997.

[18] T. Saito, T. Ninomiya, O. Isaji, T. Watanabe, H. Suzuki, and N. Okubu, "Automotive FM–CW radar with heterodyne receiver," *IEICE Trans. Commun.*, vol. E79-B, pp. 1806–1812, Dec. 1996.

[19] R. E. Zulinski and J. W. Steadman, "Idealized operation of class-E frequency multipliers," *IEEE Trans. Circuits Syst.*, vol. CAS-33, pp. 1209–1218, Dec. 1986.

[20] E. W. Bryerton, W. A. Shiroma, and Z. B. Popović, "A high-efficiency class-E oscillator," *IEEE Microwave Guided Wave Lett.*, vol. 6, pp. 441–443, Dec. 1996.

Manoja D. Weiss (S'97) was born in Colombo, Sri Lanka. She received the B.S.E.E. degree from Grove City College, Grove City, PA, in 1993, the M.S.E.E. degree from Pennsylvania State University, University Park, in 1995, and is currently working toward the Ph.D. degree in electrical engineering at the University of Colorado at Boulder.

Her research interests include microwave/millimeter-wave high-efficiency amplifiers, spatial power combining, active antennas, and microwave semiconductor devices.

Matthew H. Crites was born near Chicago, IL, in 1974. He received the B.S. degree in electrical engineering from Boston University, Boston, MA, in 1996, the M.S. degree in electrical engineering from The University of Michigan at Ann Arbor, in 1998, and is currently working toward the Ph.D. degree.

He is currently with the Center for Ultrafast Optical Science, The University of Michigan at Ann Arbor. His research interests include using ultrafast optics to examine the effects of space radiation on electronic devices.

Mr. Crites is a member of Tau Beta Pi.

Eric W. Bryerton (S'95–M'99) was born in Chicago, IL on May 30, 1974. He received the B.S.E.E. degree from the University of Illinois at Urbana-Champaign, in 1995, and the M.S.E.E. and Ph.D. degrees in electrical engineering from the University of Colorado at Boulder, in 1997 and 1999, respectively.

He is currently with the National Radio Astronomy Observatory Central Development Laboratory, Charlottesville, VA, where he is involved with millimeter-wave multiplier and amplifier design for the Atacama Large Millimeter Array (ALMA).

John F. Whitaker (S'84–M'88) received the B.Sc. degree in physics from Bucknell University, Lewisburg, PA, in 1981, and the M.Sc. and Ph.D. degrees in electrical engineering from the University of Rochester, Rochester, NY in 1983 and 1988, respectively.

In 1989, he joined the faculty of the Department of Electrical Engineering and Computer Science, The University of Michigan at Ann Arbor. He is currently a Research Scientist and Adjunct Associate Professor, as well as Coordinator of the Ultrafast Technology Area, National Science Foundation Center for Ultrafast Optical Science. In 1995 he was also a Visiting Professor, First Class, at the University of Savoie, Savoie, France. His research interests involve ultrafast-response optoelectronic materials, devices, and test and characterization techniques, and he has been extensively involved in the field of guided and free-space radiating, terahertz-bandwidth pulses.

Dr. Whitaker is a member of the IEEE Microwave Theory and Techniques Society (MTT-S) and IEEE Laser and Electro-Optics Society (LEOS). He is currently chair of the IEEE LEOS Technical Committee on Ultrafast Optics and Electronics. He was the recipient of the 1996 Microwave Prize presented by the IEEE MTT-S, and has also received the Research Excellence Award presented by the Department of Electrical Engineering and Computer Science, The University of Michigan at Ann Arbor, and the Outstanding Research Scientist Achievement Award, College of Engineering, The University of Michigan at Ann Arbor.

Zoya Popović (S'86–M'90–SM'99), for biography, see this issue, p. 2573.